Supporting Information

Scalable Synthesis of Biodegradable Black Mesoporous Silicon Nanoparticles for Highly Efficient Photothermal Therapy

Wujun Xu, [1, †,*] Konstantin Tamarov,[1, 2, †] Li Fan,[3,*] Sari Granroth,[4] Jimi Rantanen,[1] Tuomo Nissinen,[1] Sirpa Peräniemi,[5] Oskari Uski,[6] Maija-Riitta Hirvonen,[6] Vesa-Pekka Lehto[1,*]

[1] Department of Applied Physics, University of Eastern Finland, 70211, Kuopio, Finland

[2] M.V. Lomonosov Moscow State University, Faculty of Physics, 119991, Moscow, Russia

[3] Department of Pharmaceutical analysis, School of Pharmacy, and The State Key Laboratory of Cancer Biology (CBSKL), The Fourth Military Medical University, 169th Changle West Road, Xi'an, Shaanxi, 710032, China.

[4] Department of Physics and Astronomy, University of Turku, 20014, Turku, Finland

[5] School of Pharmacy, University of Eastern Finland, 70211, Kuopio, Finland

[6] Department of Environmental and Biological Sciences, University of Eastern Finland, 70211, Kuopio, Finland

[†] W. Xu and K. Tamarov contributed equally to this work.

Corresponding authors: wujun.xu@uef.fi (W. Xu); xxfanny@fmmu.edu.cn (L. Fan); vesa-pekka.lehto@uef.fi (V-P. Lehto)
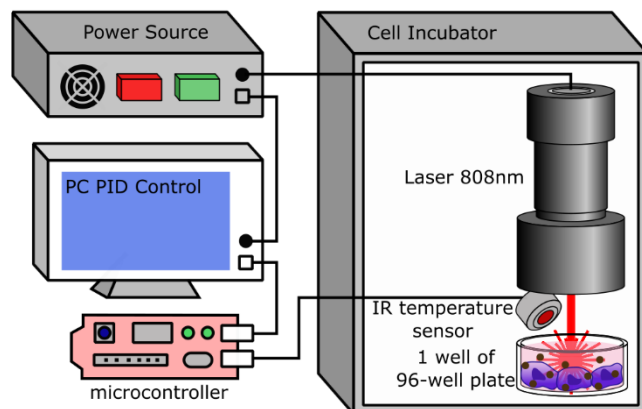
Figure S1. The schematics of the temperature-controlled laser heating for *in vitro* cell tests. The microcontroller operated the IR sensor, which read the temperature from the cell media and sent the data to the computer. The computer used the data to calculate the electrical current value to be sent to the power source, which in turn controlled the power of the laser irradiation.
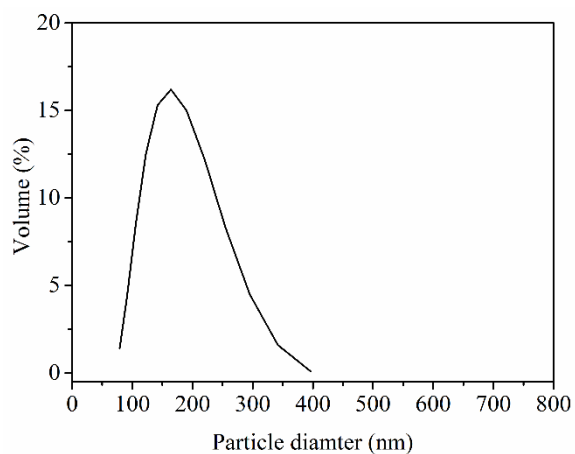

Figure S2. Particle diameter distribution of BPSi measured with the DLS. The nanoparticles were dispersed in deionized H_2O prior to the measurement.

Calculation of porosity of BPSi

The total volume of the sample $V_{tot}=V_{Si} + V_{pore}$, where V_{Si} is the volume of silicon and V_{pore} is the pore volume of the sample and measured value is 0.42 cm^3/g according to the N_2 ad/desorption measurements.

Also, the total volume of the same $V_{tot}=m_{tot}/d_{tot}$, where m_{tot} is the mass of the sample and d_{tot} is the density of the sample. If we use 1g as total mass of the BPSi, the mass of silicon in the sample is 1.0 because the air mass filled in the pores is negligible (Density of air at 20 °C at standard pressure is $1.2*10^{-3}$ g/cm^3). The density of silicon is $d_{Si}=2.329$ g/cm^3. So, the total volume of the sample is 0.85 cm^3.

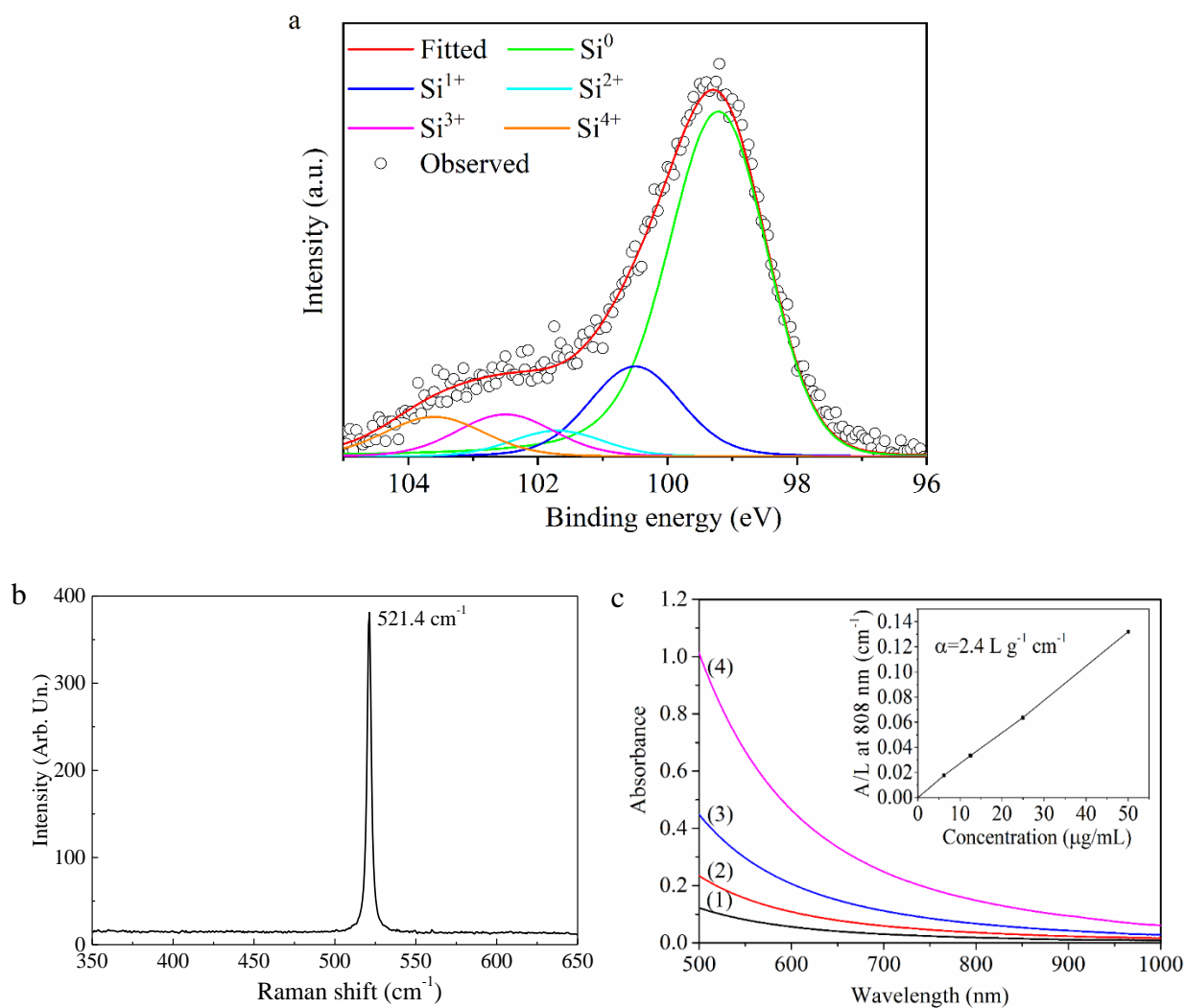So, the porosity of the sample= V_{pore}/V_{tot}=0.42/0.85=49.4%.

Figure S3. (a) Si 2p spectrum *e*PSi powder obtained in XPS analysis, (b) Raman spectrum of bulk silicon wafer, and (c) UV-Vis extinction spectra of *e*PSi nanoparticles in aqueous solutions (Concentration of the nanoparticles: (1) 6.25 μg/ml, (2) 12.5 μg/ml, (3) 25.0 μg/ml, and (4) 50.0 μg/ml). The inset shows the normalized absorbance intensity (A) divided by the characteristic length (L) of the cell at 808 nm for solutions shown in (c). The mass extinction coefficient (α) at 808 nm was calculated to be 2.4 L g^{-1} cm^{-1}, according to the Lambert-Beer Law.

Table S1. Fitted area percentage of different silicon (Si) species in XPS analysis

	elemental Si^0 (%)	Si^{1+} (Si_2O) (%)	Si^{2+} (SiO) (%)	Si^{3+} (Si_2O_3) (%)	Si^{4+} (SiO_2) (%)
*e*PSi	64	11	6	9	10
BPSi	54	3	5	14	24

Table S2. Sample information of the nanoparticles for photothermal heating tests.

	Diameter	Shape	Concentration (μg/mL)	Manufacturer
Fe3O4	10 nm	Sphere	50	Prepared based on reference[1]
Au	5 nm	Sphere	50	Sigma (product number 741949)
	80 nm	Sphere	50	Sigma (product number 742023)
	150	Sphere	50	Sigma (product number 742058)
Carbon nanotube (CNT)		Single wall nanotubes	50	Timesnano (www.timesnano.com)

Calculation of optical bandgap.

The calculation of optical bandgap was done using the UV-Vis absorption spectra according to the Kubelka-Munk model[2]. Briefly, in this model, the increase of absorption is approximated with a linear equation, whose intercept with X axis represents the value for the bandgap. Figure S5 shows the results for 28 μg/ml suspensions of ePSi and BPSi NPs. The calculated values are 2.51 eV and 1.34 eV for ePSi and BPSi NPs, respectively.
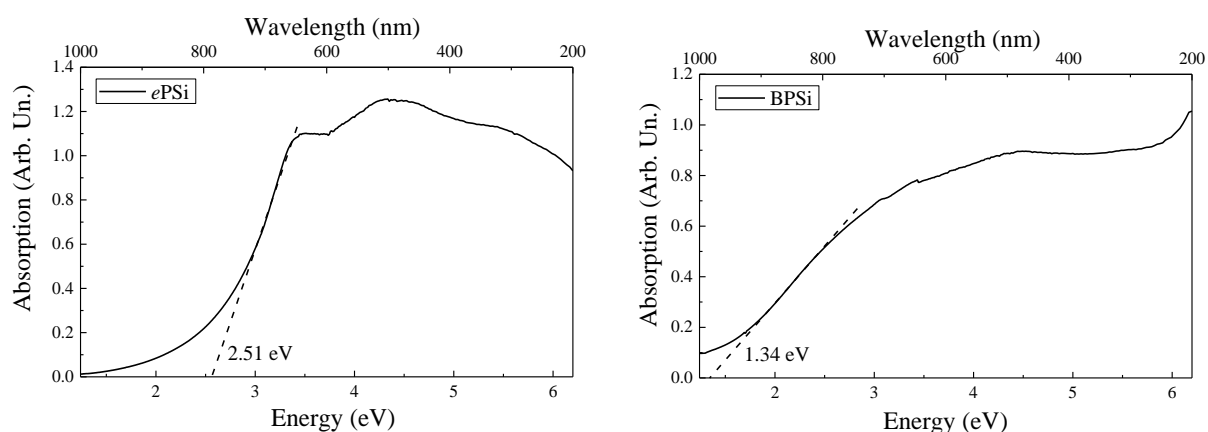

Figure S4. The optical bandgap calculations according to the Kubelka-Munk model for ePSi (left) and BPSi (right). Both the ePSi and BPSi have the concentration of 28 μg/ml.
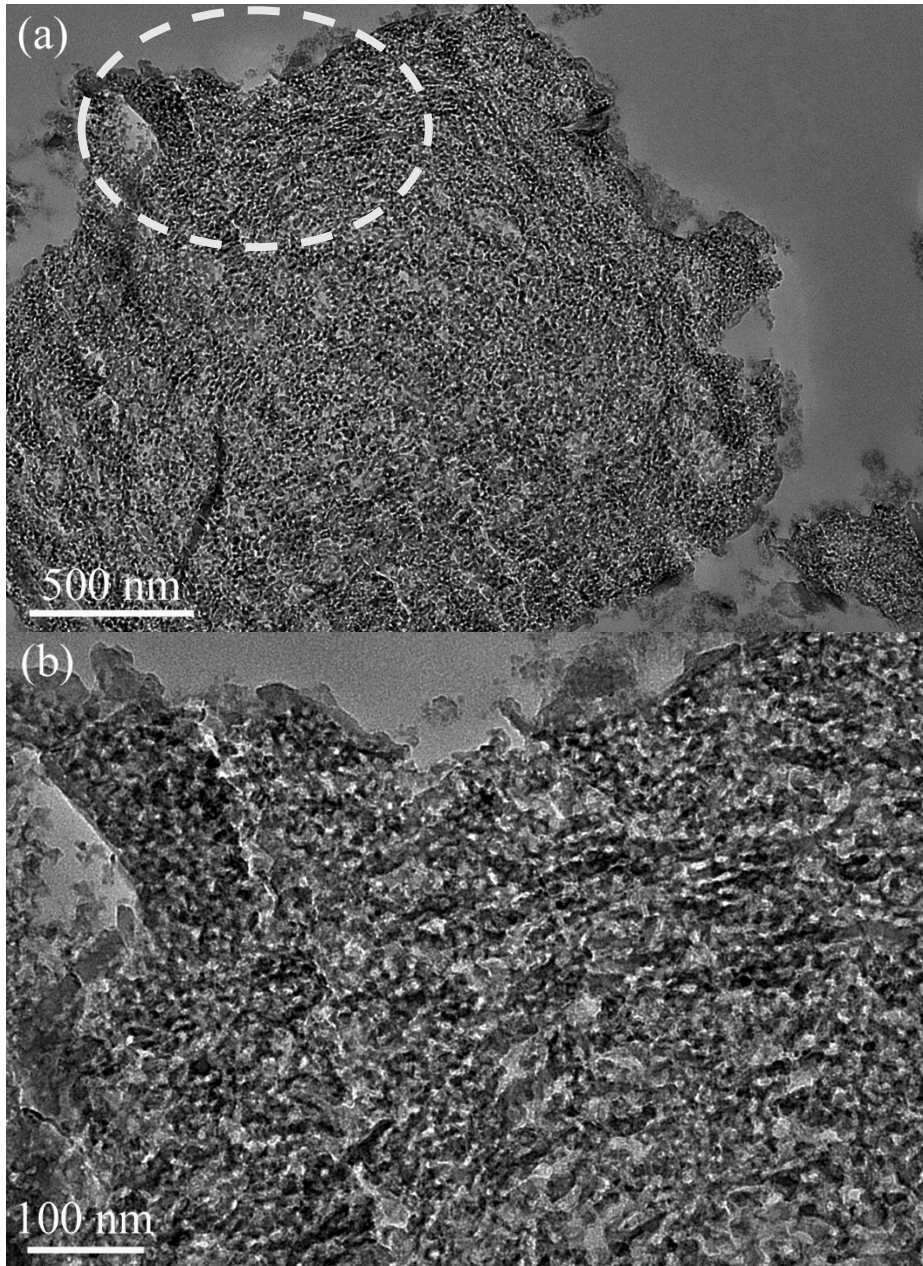
Figure S5 TEM images of BPSi slices prepared from the microparticles. The image of (b) was taken from the circle-marked area in image (a).The porous structure is clearly observed in the BPSi microparticles.
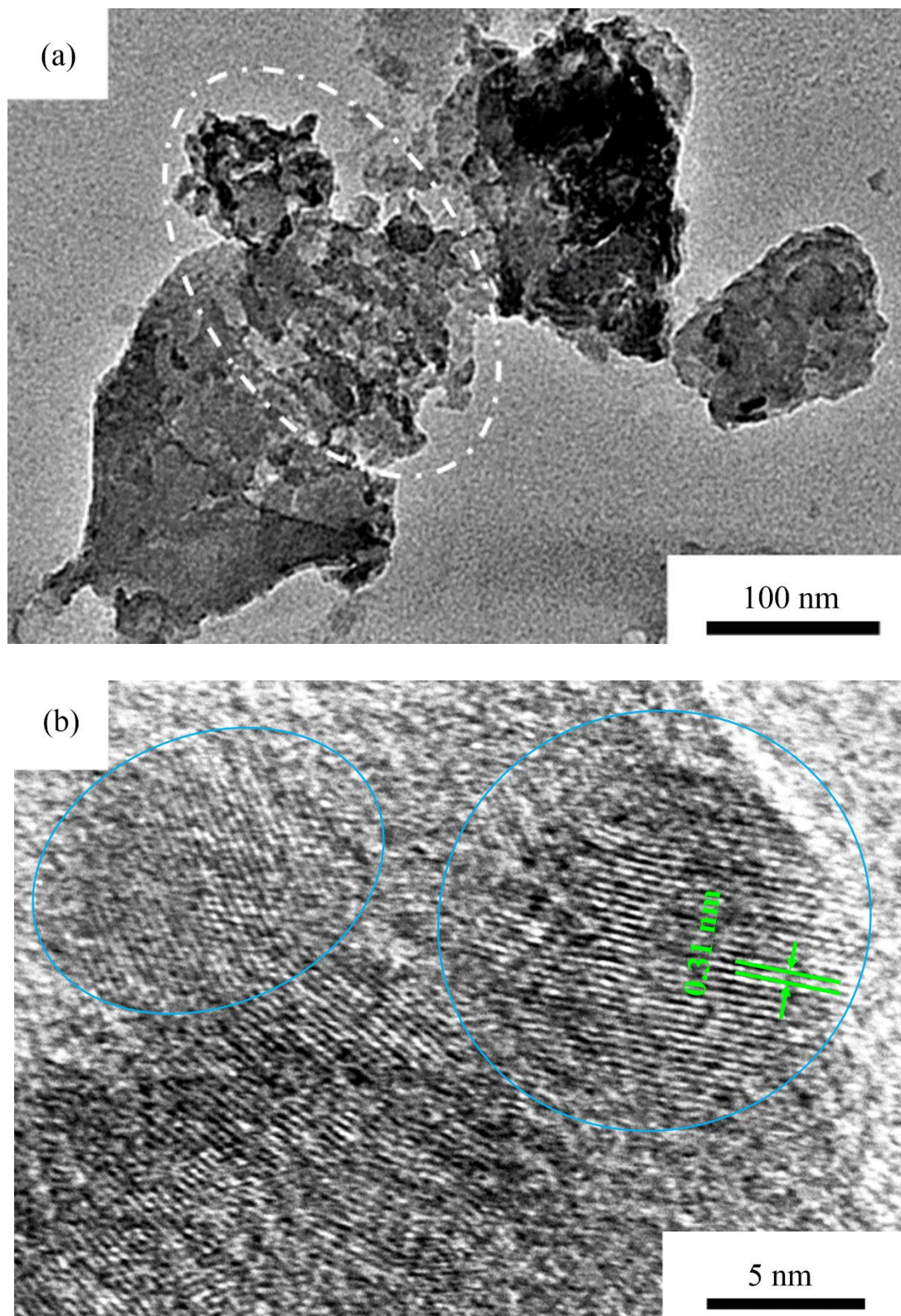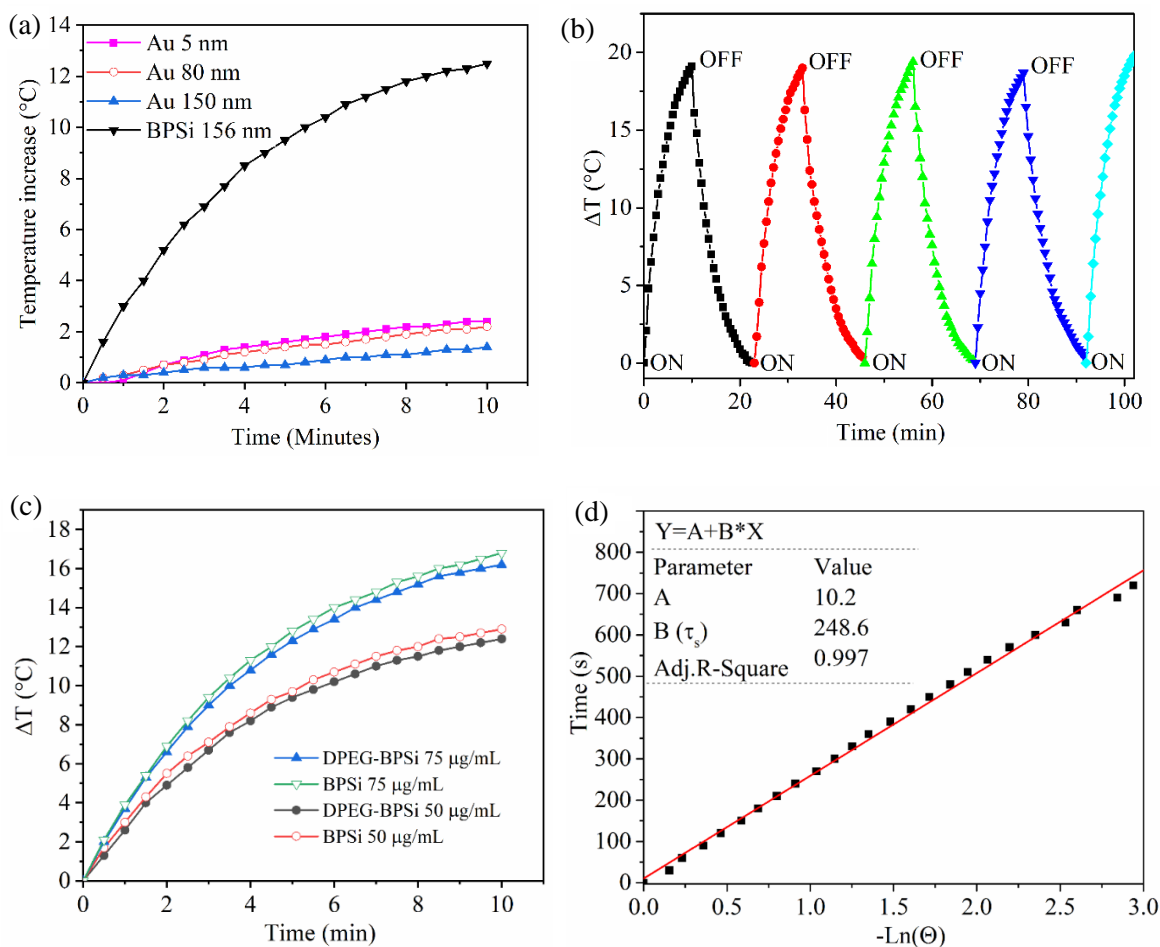
Figure S6 (a) Low magnification TEM image of BPSi. Porous structure is observed in the selected area. (b) High resolution (HR)-TEM image of BPSi. The crystallite size of the nanoparticles is between 10 and 20 nm according to the estimation from blue circle.

Figure S7. (a) Heating performance comparison of BPSi nanoparticles with gold nanoparticles with different sizes. The concentration of the nanoparticles was 50 µg/mL and 808 nm laser (1.0 W) was used for the test. (b) Photostability tests: The aqueous solution of BiPSi nanoparticles (100 ug/ml) was irradiated with five cycles of heating (laser on)-cooling (laser off) process. The sample solution was cooled to ambient temperature (25 °C) with the ambient air in fume hood during the laser off period. (c) Heating performance of the BPSi nanoparticles with and without PEG coating with NIR laser irradiation (808 nm, 1.0 W). BPSi and DPEG-BPSi had the corresponding silicon content if the samples had the same particle concentration. (d). Linear time data versus -lnθ obtained from the cooling period of Figure S7b.

Calculation of photothermal conversion efficiency:

The photothermal conversion efficiency (η) of BPSi at 808 nm was calculated according to the reported method using the following equations[3-4]:

$$\eta = \frac{hs(T_{max} - T_{max,water})}{I(1 - 10^{-A_{808}})} \quad (1)$$

$$hs = \frac{mC_p}{\tau_s} \quad (2)$$

$$\tau_s = -\frac{t}{\ln(\theta)} \quad (3)$$

$$\theta = \frac{T_{amb} - T}{T_{amb} - T_{max}} \quad (4)$$

where h is heat transfer coefficient, s is the surface area of the container, T_{max} is the equilibrium temperature of the sample solution after laser heating, $T_{max,\ water}$ is the equilibrium temperature of pure water under laser heating, I is the laser power density (1.0 W). A_{808} is the absorbance of the sample at 808 nm. m is the mass of product, C_p is specific heat capacity of dispersing agent, H_2O (C_p, 4.2 J/(g·°C)). 1.0 mL aqueous dispersion of BPSi was used in the test and so m is 1.0 g (mass of sample solution). A_{808} is 1.32 when the concentration is 100 µg/ml. τ_s is obtained from Figure S7d, which is calculated based on the data from the cooling period of Figure S7b.
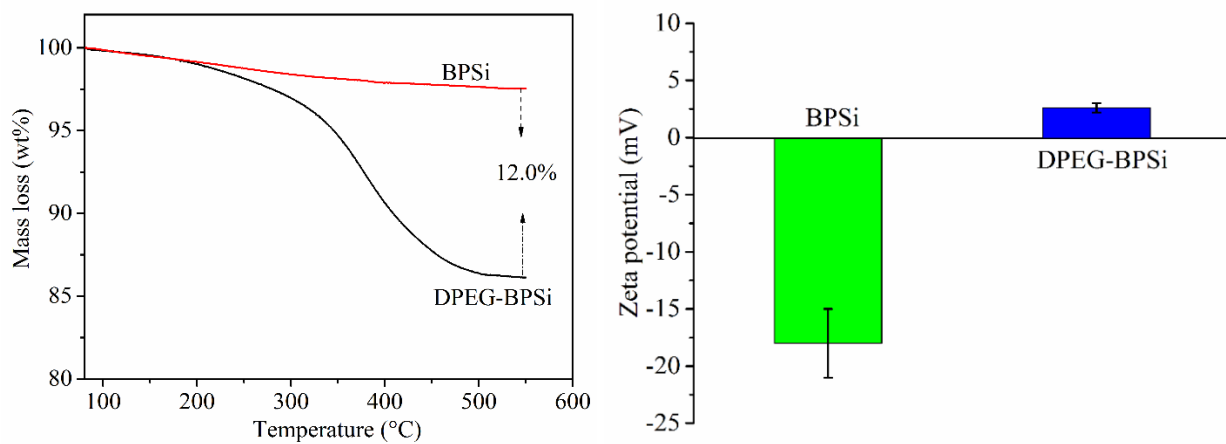
Figure S8. TG curves (left) and zeta potential (right) of nanoparticles. The surface charges of the nanoparticles were measured in 1:1 diluted PBS at pH 7.4.
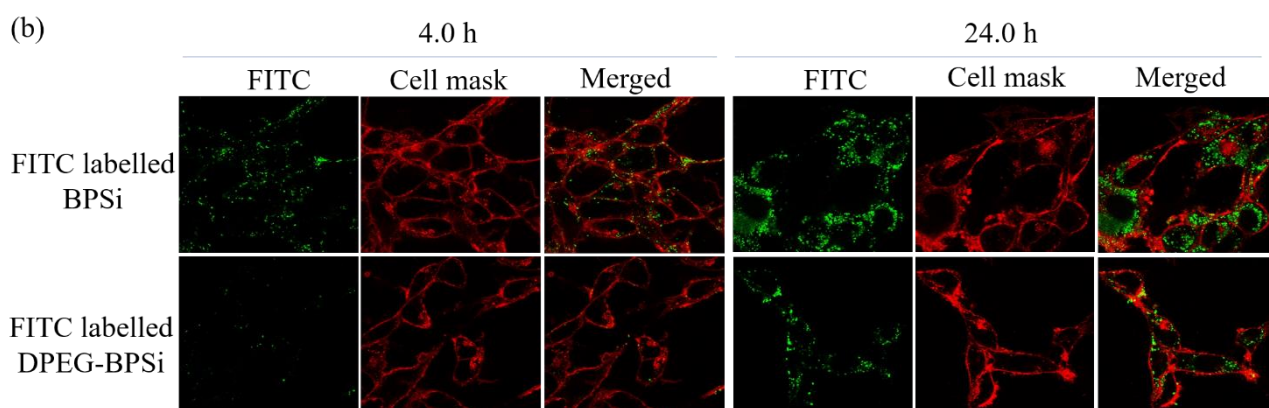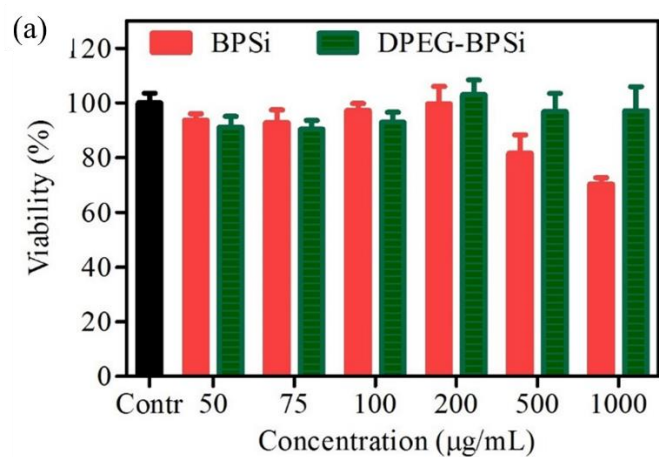
Figure S9. (a) Cell viability of CT26 cells. The different concentrations of BPSi and DPEG-BPSi nanoparticles were incubated with the cells for 4 hours and then the cells were washed with cell medium. The cell viability was analyzed with CellTiter Glo assay after the additional 44 hours' incubation. (b) Cell uptake of FITC labeled BPSi and DPEG-BPSi nanoparticles after the incubation of 4.0 h and 24.0 h. The nanoparticles and cell membrane were labeled separately with FITC and Cellmask for fluorescent confocal microscope image.
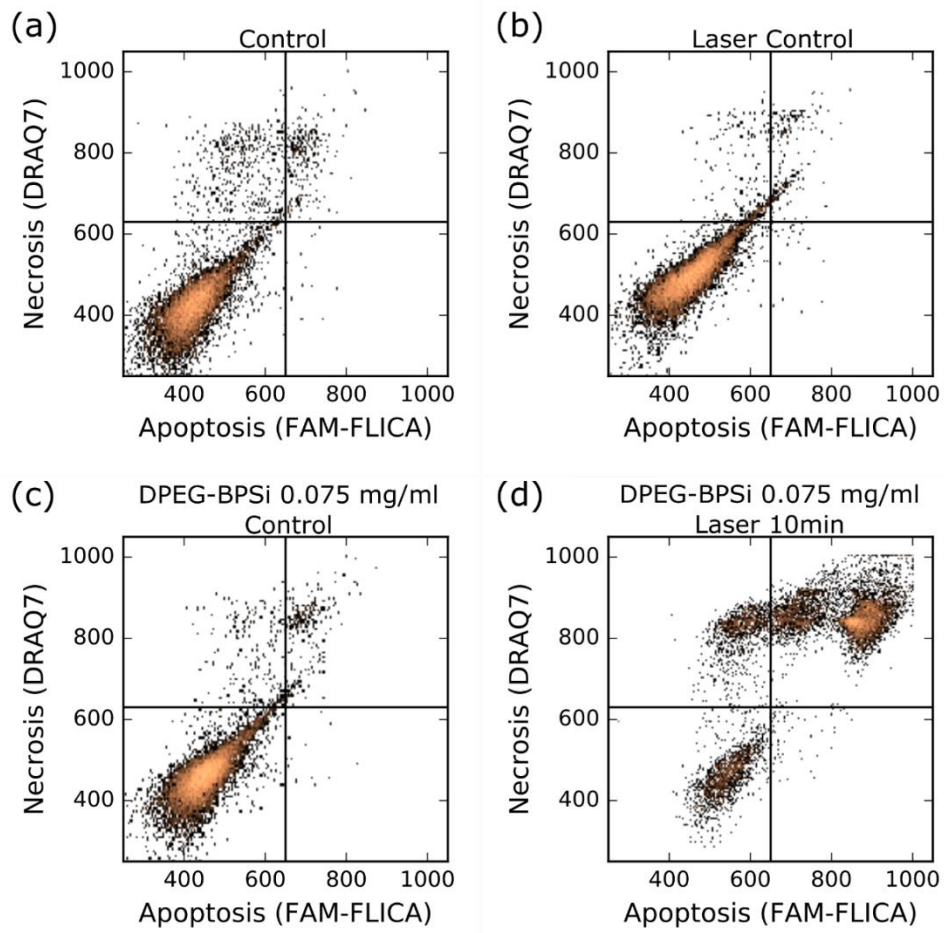
Figure S10. 2D plots of cell populations from flow cytometry measurements. The quarters represent live cells (q1); apoptotic cells (q2); late apoptotic cells (q3) and necrotic cells (q4). The evaluation of CT 26 cell populations after 10 min laser full power laser heating in the presence of 0.075 mg/ml of DPEG-BPSi NPs after 12 hours of post treatment incubation time: (a) Control cells without laser treatment, (b) Control cells with laser treatment only, (c) Control cells treated with DPEG-BPSi nanoparticles only, (d) Cells treated with both DPEG-BPSi nanoparticles and the laser.
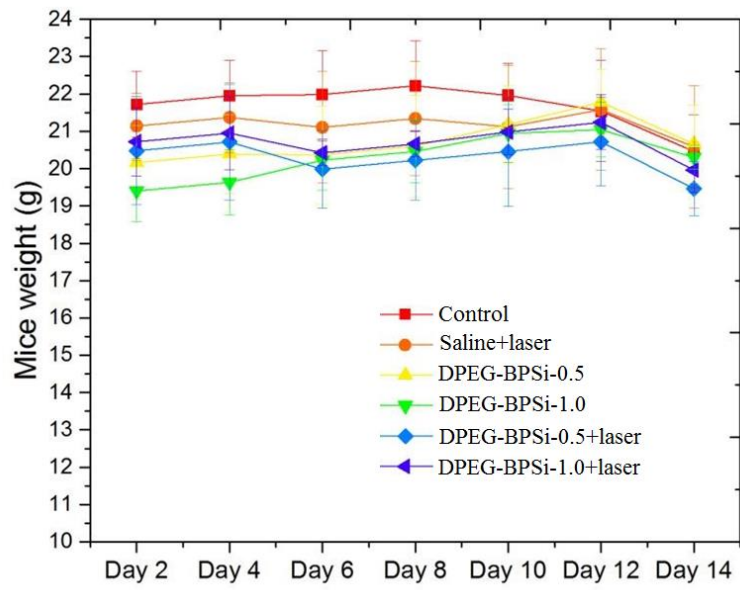
Figure S11. Body weight changes in colonic tumor bearing mice during the 14-day experiment period (mean ± SD, n=5). No Significant difference of body weight change according to the one-way ANOVA statistical analysis.
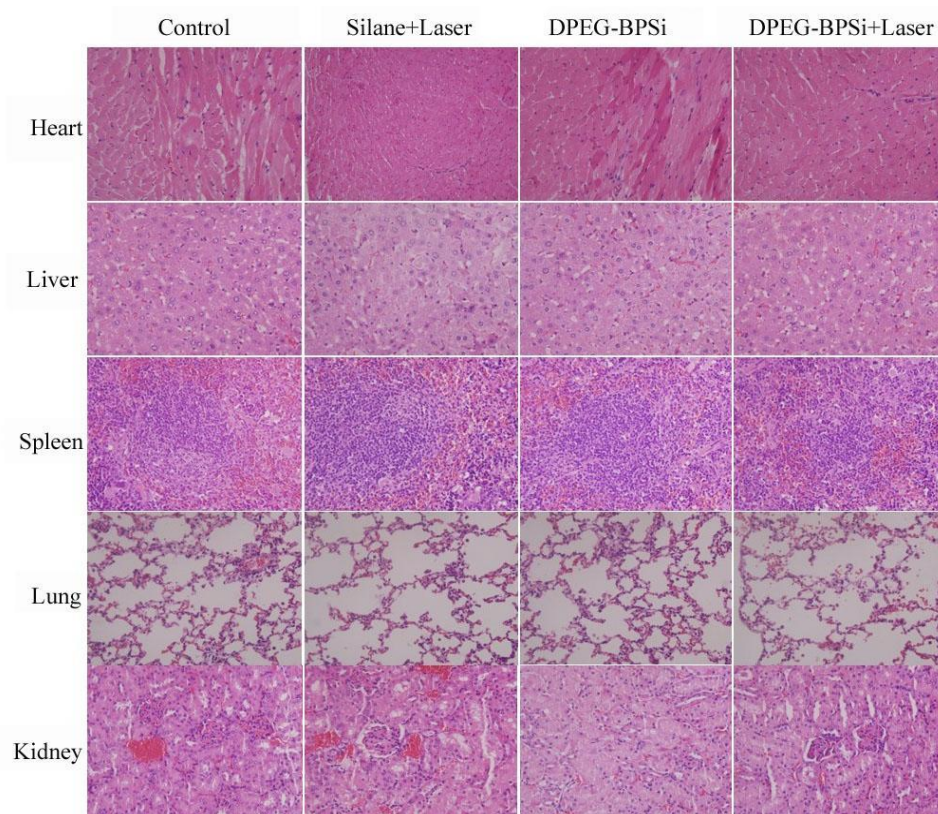
Figure S12. H&E stained images of the heart, liver, spleen, lung and kidney in control and treatment groups in mice bearing CT26 cells. The concentration of the intratumorally injected nanoparticles is 1.0 mg/mL.

References:

(1) Wan, J.; Cai, W.; Meng, X.; Liu, E. Monodisperse Water-Soluble Magnetite Nanoparticles Prepared by Polyol Process for High-Performance Magnetic Resonance Imaging. *Chem. Commun.* **2007,** *47*, 5004-5006.
(2) Murphy, A. Band-Gap Determination from Diffuse Reflectance Measurements of Semiconductor Films, and Application to Photoelectrochemical Water-Splitting. *Sol. Energy Mater. Sol. Cells* **2007,** *91*, 1326-1337.
(3) Roper, D. K.; Ahn, W.; Hoepfner, M. Microscale Heat Transfer Transduced by Surface Plasmon Resonant Gold Nanoparticles. *J. Phys. Chem. C* **2007,** *111*, 3636-3641.
(4) Sun, C.; Wen, L.; Zeng, J.; Wang, Y.; Sun, Q.; Deng, L.; Zhao, C.; Li, Z. One-Pot Solventless Preparation of Pegylated Black Phosphorus Nanoparticles for Photoacoustic Imaging and Photothermal Therapy Of cancer. *Biomaterials* **2016,** *91*, 81-89.